ARTICLE

Porous Organic Crystals Crosslinked by Free-radical Reactions

Krishanu Samanta,¹ Jiashan Mi,^{2, 3} Albert D. Chen,¹ Fangzhou Li,⁴ Richard J. Staples,⁵ Aaron J. Rossini,^{2, 3} Chenfeng Ke^{1, 4, *}

Received 00th January 20xx, Accepted 00th January 20xx

DOI: 10.1039/x0xx00000x

Two hydrogen-bonded crosslinked organic frameworks (H_cOFs) were synthesized via free radical reactions utilizing butadiene and isoprene as crosslinkers. These H_cOFs exhibit high crystallinity, enabling detailed structural characterization via single-crystal X-ray diffraction analysis. Subsequently, one of the olefin-rich H_cOFs was converted to a hydroxylated framework through hydroboration-oxidation while maintaining the high crystallinity.

Porous materials¹ are attractive for their diverse applications for substrate storage and separation,² catalysis,³ ion transport,⁴ and sensing.⁵ Among these materials, crystalline organic frameworks like metal-organic frameworks (MOFs),6 covalent organic frameworks (COFs),⁷ and hydrogen-bonded organic frameworks (HOFs)⁸ have been extensively investigated for their adjustable pore characteristics via building block variation. Establishing a fundamental understanding of the structure-property relationship between the framework materials and their substrates hinges on atomic-level details obtainable through single-crystal X-ray diffraction (SCXRD).9 Furthermore, achieving high chemical stability in these frameworks is crucial for their application in various environments. 10 However, enhancing chemical robustness and maintaining structural detail often presents a trade-off due to the required reversible bond formation processes during the synthesis of these framework

Recently, hydrogen-bonded crosslinked organic frameworks (H_COFs) have emerged, featuring balanced high crystallinity and chemical stability.¹¹ The synthesis of H_COFs involves the design

of molecular building blocks with hydrogen bonding direction groups and reactive arms. These building blocks self-assemble via hydrogen bonds in the solid state to form potentially porous networks. Unlike HOFs, these networks do not require high stability after solvent removal because the subsequent photocrosslinkings with dithiol through the irreversible thiol-ene or thiol-yne reactions reinforce them as H_COFs. These H_COFs showed high performance in iodine/iodide removal in water purification,¹² serve as solid-state hosts for photo-switching,¹³ and facilitate boron trifluoride uptake for cationic vinyl ether polymerizations.¹⁴ However, the synthesis of H_COFs has been limited to thioether crosslinked variants. Diversifying the crosslinking methods could significantly broaden the potential applications for H_COFs.

In this study, we unveiled a new approach to synthesize singlecrystalline H_COFs through free radical crosslinking. By integrating styrene groups into the carboxylic acid-based monomer, we achieved co-crystallization of the monomer with triallyl-benzamide (TAB) through complementary hydrogenbonding interactions. This self-assembly process produced porous co-crystals, which were subsequently subjected to free radical reactions in the presence of butadiene and isoprene, resulting in crosslinked crystalline organic frameworks H_COF-106 and H_COF-107 (Scheme 1). Interestingly, the reaction occurred among the diene crosslinker, the styrene units, and the allyl groups, yielding crosslinked H_COFs. The abundant olefin groups at the pore surfaces facilitated the further modifications of H_COF-107, transforming its hydrophobic pore surface into a hydrophilic one through hydroboration-oxidation. modification of the pore surface inversely affected the vapor sorption properties of these H_COFs, demonstrating the versatility of post-synthetic modification approach¹⁵ in tailoring material properties for specific vapors.

We chose tris-(4-carboxyl phenyl)-benzene and TAB (Scheme 1) as the building blocks because they co-crystallized as a hydrogen-bonded network with large pores in the solid state as we reported recently. ¹⁶ The styrene moieties are introduced to monomer 1 in four steps (Scheme S1). Firstly, methyl-4-bromo-

Email: cke@wustl.edu

¹ Department of Chemistry, Dartmouth College, 41 College Street, Hanover, NH 03755, USA

² Department of Chemistry, Iowa State University, 2438 Pammel Drive, Ames, IA 50011, USA

³ US DOE Ames National Laboratory, Ames, Iowa, USA, 50011

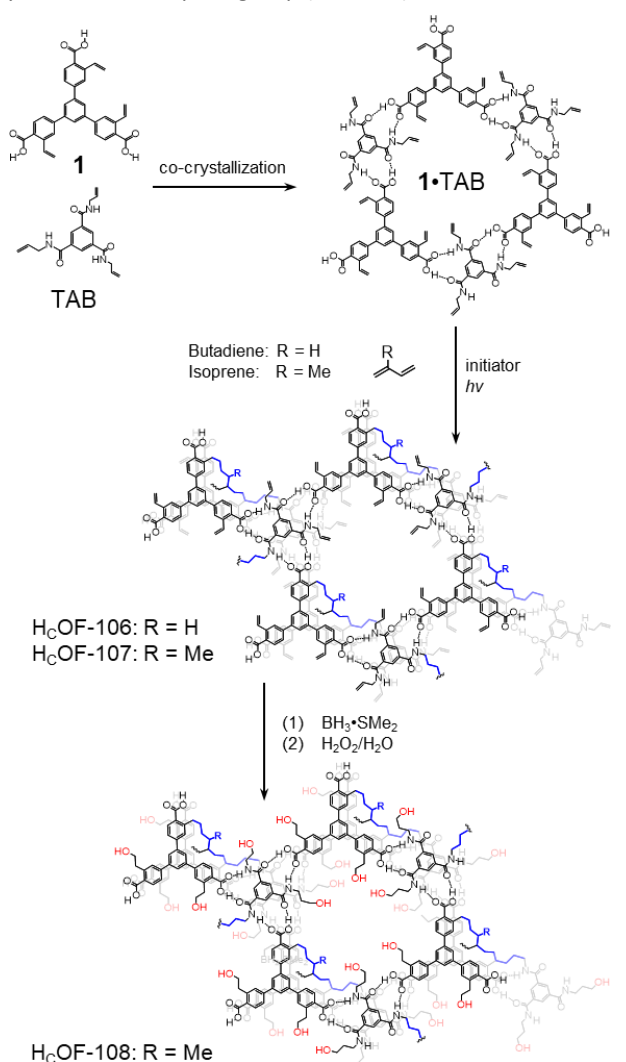
⁴ Department of Chemistry, Washington University in St. Louis, One Brookings Drive, St. Louis, MO 63130, USA

⁵ Department of Chemistry, Michigan State University, 578 S. Shaw Lane, East Lansing, MI 48824, USA

ARTICLE Journal Name

2-bromomethylbenzoate was converted to methyl-4-bromo-2-vinylbenzoate through the Wittig reaction.¹⁷ It then reacted with 1,3,5-phenyltriboronic tris(pinacol)ester via Suzuki-Miyaura coupling followed by hydrolysis to generate monomer **1** in 49% overall yield.

Slow vapor diffusion of hexane or cyclohexane into the dioxane solution of monomer $\bf 1$ and TAB 1:1 mixture for 7 days afforded needle-shaped co-crystals suitable for SCXRD analysis (Fig. 1). In the solid state, monomer $\bf 1$ and TAB formed 1:1 co-crystals in the $P\overline{\bf 1}$ space group (Table S2). In this $\bf 1 \bullet TAB$



Scheme 1. Synthesis of $H_cOF-106$ and $H_cOF-107$ through free-radical reactions with butadiene and isoprene. Post-modification of the single-crystalline $H_cOF-107$ affords its hydroxylated derivative $H_cOF-108$.

co-crystal, the carboxylic acid groups of **1** form highly directional hydrogen bonds with the benzamide via a donor-acceptor to donor-donor-acceptor (DA-D_DA) hydrogen bonding array. This array repeats among the three carboxylic acid groups of **1**, forming a 2D hexagonal hydrogen bonding sheet along the b/c plane (Fig 1a). These 2D hexagonal layers are stacked in a nearly eclipsed manner, forming 1D channels along the a-axis with pore aperture measured as $13.3 \times 11.1 \, \text{Å}^2$ and 32% solvent-filled voids (Fig. 1a). Along the direction of the pores, monomer **1** and TAB are stacked with an alternative ABBA fashion, with the π - π

distance measured as 3.7, 4.2, and 3.5 Å (Fig. 1b). Three sets of styrene groups of 1 in adjacent layers are packed close to each other with measured olefin-to-olefin distances as 3.83, 8.4, and 9.21 Å (Fig. 1b). In comparison, the closest olefin-to-olefin distance in the 2D layer is measured as 13.5 Å (Fig. S29a). The various olefin distances in the 1•TAB co-crystal could result in different reactivities for free-radical crosslinking. We also measured the styrene to allyl group distances with the intra-2D-layer distances of 4.26–4.65 Å (Fig. S29c) and inter-2D-layer distances of 3.63–7.86 Å (Fig. S29d). Therefore, we chose butadiene and isoprene as the crosslinkers to connect these olefin groups in the 1•TAB co-crystal for H_COF synthesis. Their versatile reactivity for 1,2- or 1,4-addition may accommodate different olefin-to-olefin distances in the co-crystal.

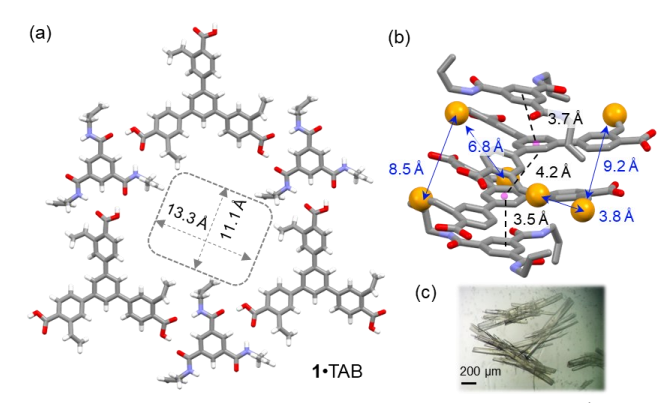


Fig. 1 (a) Single-crystal structure of the $1 \cdot TAB$ co-crystal viewed along the b/c plane. (b) The ABBA-type alternative packing of 1 and TAB, viewed along the a-axis. The π - π stacking distances and distances between the terminal carbon atoms of the styrene moieties are highlighted. (c) The optical image of $1 \cdot TAB$ co-crystals.

The 1•TAB co-crystals were washed extensively using hexane and then soaked in the butadiene hexane solution (15 w/w%) or neat isoprene, along with a photo-initiator 2,2-dimethoxy-2phenylacetophenone (DMPA, 0.04 mol % to diene), for 24 h in the dark to allow extensive diffusion of dienes. The reaction vials were photo-irradiated for 48 h under the UV lamp. Interestingly, we didn't observe significant amounts of polybutadiene or polyisoprene generated in solution or the neat phase, and the diene conversion ratio for free radical reaction outside the cocrystals was too low to be detected by ¹H NMR spectroscopy (Fig. S23-S24). The obtained crystals were washed to remove the unreacted dienes and soaked in boiling DMSO-d₆. After cooling down, a majority of the crystal samples remained insoluble (Fig. S12). However, soluble residues account for unreacted or partially reacted monomer 1 and TAB were detected in the 1H NMR spectra (Fig. S13-S14). Using gravimetric analysis, approximately 60 wt% and 70 wt% of the co-crystals were estimated as crosslinked by butadiene and isoprene, respectively. The afforded H_COF-106 and H_COF-107 (Scheme 1) were subjected to various spectroscopic analyses. In the FT-IR spectra, unreacted olefin groups attributed to 1 and TAB monomers were observed (Fig. S15). Compared to the Solidstate ¹³C NMR spectrum of **1**•TAB, carbon signals attributed to the styrene moieties and allyl groups were reduced (Fig. 2, Table S5). The addition of butadiene and isoprene crosslinkers was evident as the carbon signals for methylene units at around 25**Journal Name** ARTICLE

signals for methyl groups originating from the isoprene were found at 15 ppm for H_COF-107 (Fig. 2).

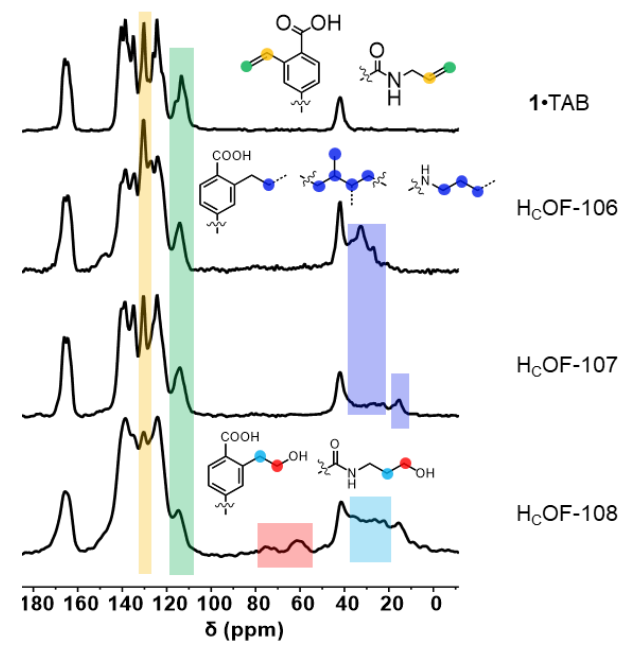


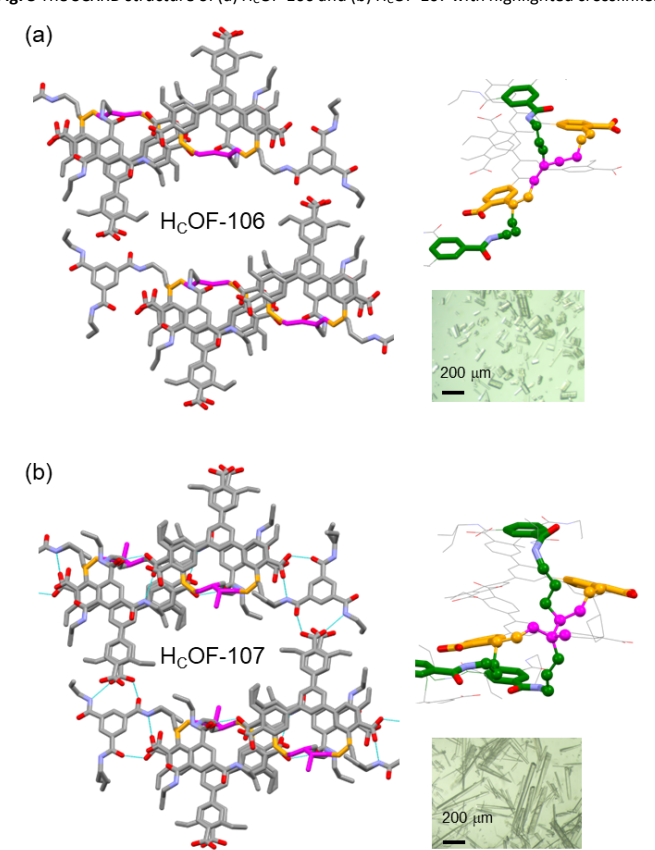
Fig. 2 Stacked solid-state 13 C NMR spectra of 1•TAB, H_COF-106, H_COF-107, and H_COF-108 from top to bottom, respectively.

Powder X-ray diffraction (PXRD) analysis showed that H_COF-106 and H_COF-107 remained highly crystalline (Fig. S22), and both are suitable for SCXRD analysis. Compared to 1. TAB, H_COF-106 and H_COF-107 possess the same P1 space group and their unit cell volumes only expanded by 3% after the free-radical reaction (Table S2). SCXRD analysis of HcOF-106 and HcOF-107 revealed that 50% of styrene units in 1 and 50% of allyl groups in TAB took part in crosslinking, resulting in residual olefins in the crystal lattice. To confirm this, we subjected H_COF-107 to the iodine value test following the Wijs method. 18 Compared to the iodine value of 181 for the 1 • TAB co-crystal, the iodine values of H_COF-107 decreased to 88, confirming the number of olefin groups decreased by ~50% after crosslinking.

The hydrogen-bond pattern remained unchanged in HcOF-106 and $H_{\text{C}}\text{OF-107}$, along with the hexagonal pore structure (Fig. 3). After crosslinking, the pore apertures of HcOF-106 and HcOF-107 decreased to 11.2 \times 10.5 Å² and 11.2 \times 10.9 Å², respectively (Fig. S32c and S30c). In $H_{\text{c}}\text{OF-106}$, the butadiene reacted with two styrene groups present in consecutive layers via 1,4addition, and one of the styrene reacted with allyl groups (Fig. 3a). Similar crosslinking pattern was also observed for HcOF-107 (Fig. 3b). These interlayer connections forms stable crosslinked frameworks. We suspect that the allyl groups of TAB might act as a radical chain transfer agent during crosslinking, which enabled the subsequent addition of the second allyl group to the C2 position of the butadiene or isoprene. To confirm the reaction that took place between allyl groups and styrene/diene, we synthesized a control co-crystal using triethylbenzamide (TEB) and monomer 1. The 1•TEB co-crystal showed a nearly identical hydrogen-bonded network to 1 • TAB (Table S2 and Fig. S33). When the 1. TEB co-crystal was reacted with

40 ppm were found for both H_COF-106 and H_COF-107. Carbon isoprene, the obtained crystals were largely dissolved in DMSO d_6 (Fig. S35). ¹H NMR spectrum of the dissolved sample showed that ~40% of 1 remained unreacted (Fig. S36). This result confirmed that the allyl groups participated in the crosslinking reaction, although the detailed reaction path remains ambiguous (Scheme S5).

 $\textbf{Fig. 3} \ \text{The SCXRD structure of (a)} \ H_{\text{C}} \text{OF-106 and (b)} \ H_{\text{C}} \text{OF-107 with highlighted crosslinkers}$



(magenta) in the crystal lattices. The crosslinking connections between the layers in H_COF-106 and H_COF-107 are shown on the right. Inset: Optical images of these crystals.

The rich olefin contents at the pore surface of these H_COFs encouraged us to post-synthetically convert the olefins to hydroxyl groups while maintaining the material's high crystallinity. This post-modification will enable us to convert the hydrophobic pore surface to a hydrophilic pore surface. To illustrate this feasibility, we chose H_COF-107 as the model material for the subsequent modifications. As shown in Scheme 1, single crystals of H_COF-107 were immersed in BH₃•SMe₂ for 24 h to allow extensive hydroboration, and the crystals turned pink after the reaction. ^{11}B NMR spectra of $H_{c}OF-107-BH_{2}$ showed signals characteristic of boronic acid (Fig. S39), suggesting that the -CBH2 • SMe2 units are highly reactive and readily hydrolyzed or oxidized. $H_{\text{C}}\text{OF-108}$ was obtained by reacting H_COF-107-BH₂ with water and H₂O₂ to ensure full oxidation of any residual boronic esters. The H_COF-108 crystals retained high crystallinity, as shown by PXRD (Fig. 4a), but it is no longer suitable for SCXRD analysis. The ¹³C CP MAS NMR spectra showed that the carbon signals attributed to the residual alkene groups at 114 ppm decreased significantly (Fig 2, Table S5), and a new carbon signal attributed to the oxidized -CH₂OH group emerged at 64 ppm (Fig. 2). In addition, the carbon

ARTICLE Journal Name

results showed successful hydroboration-oxidation of the olefin Ames Laboratory is operated by Iowa State University for the groups, generating H_COF-108 with hydrophilic pores.

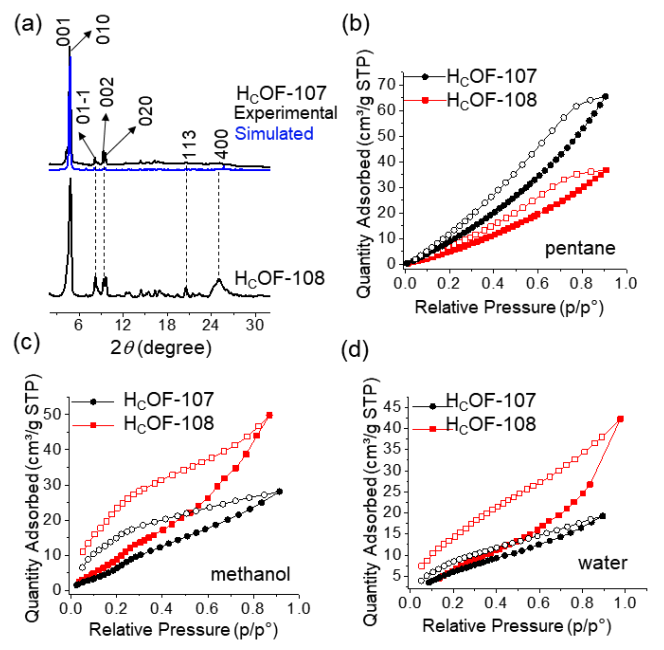


Fig. 4 (a) Simulated ($H_{c}OF-107$) and experimental PXRD patterns of $H_{c}OF-107$ and H_COF-108. (b) Pentane, (c) methanol, and (d) water vapor sorption isotherms for H_cOF-107 (black) and H_cOF-108 (red) measured at 295 K.

To confirm the pore characteristic change, solvent vapor sorption analyses were performed for H_COF-107 and H_COF-108 using nonpolar solvent pentane and polar solvents methanol and water. As shown in Fig. 4(b-d), the sequence of the solvent vapor uptake values is inversed after the post-modification. $H_COF\text{-}108$ absorbed 50 cm $^3g^{\text{-}1}$ of methanol and 36 cm $^3g^{\text{-}1}$ of pentane, in contrast to H_COF-107, which absorbed 28 cm³g⁻¹ of methanol and 66 cm³g⁻¹ of pentane (Fig. S43d). The inverted sorption feature highlights the benefit of post-modification.

In conclusion, our work has effectively demonstrated the application of free-radical crosslinking in creating hydrogenbonded crosslinked organic frameworks, yielding two HcOFs through the use of butadiene and isoprene as crosslinkers and allyl/styrene-based monomers for hydrogen-bonded network formation. The structural analysis revealed that HcOF-106 and H_COF-107 feature crosslinked networks, with the crosslinking reaction occurring among styrene groups of the carboxylic acidbased monomers, the diene crosslinkers, and the allyl groups of the triallyl-benzamide monomers. Furthermore, we successfully converted the olefin-decorated pore surface of HcOF-107 to a hydroxylated H_cOF-108 while preserving the materials' crystallinity. The opposite vapor sorption behaviors of the hydrophobic H_COF-107 and hydrophilic H_COF-108 emphasize their difference in the pore surface characteristics. The successful synthesis and post-synthetic modification of these H_COFs highlight the versatility and potential of utilizing new crosslinking methods to develop functional porous materials.

This work is supported by the National Science Foundation (NSF) CAREER award (DMR-1844920). Solid-state NMR experiments by A.J.R. were supported by the U.S. Department

signals attributed to the saturated alkyl groups increased. These of Energy (DOE), Office of Science, Basic Energy Sciences. The DOE under contract No. DE-AC02-07CH11358. Funding for the SCXRD was provided by the NSF MRI program (1919565).

Conflicts of interest

There are no conflicts to declare.

Data Availability

The data supporting this article have been included as part of the Supplementary Information. The Single-crystal X-ray Diffraction data in this report has been deposited at the Cambridge Crystallographic Data Centre (CCDC) and these data can be obtained free of charge at www.ccdc.cam.ac.uk/data_request/cif or by emailing data_request@ccdc.cam.ac.uk. CCDC deposition numbers are 2347283, 2347284, 2347291, and 2347292.

Notes and references

- (α) A. G. Slater and A. I. Cooper, Science, 2015, **348**, aaa8075; (b) R.-B. Lin, Y. He, P. Li, H. Wang, W. Zhou and B. Chen, Chem. Soc. Rev., 2019, 48, 1362-1389; (c) Y. Jin, Y. Hu and W. Zhang, Nat. Rev. Chem., 2017, 1,0056.
- (a) Z. Chen, K. O. Kirlikovali, K. B. Idrees, M. C. Wasson and O. K. Farha, Chem, 2022, 8, 693–716; (b) Z. Wang, S. Zhang, Y. Chen, Z. Zhang and S. Ma, Chem. Soc. Rev., 2020, 49, 708-735.
- S. Lin, C. S. Diercks, Y.-B. Zhang, N. Kornienko, E. M. Nichols, Y. Zhao, A. R. Paris, D. Kim, P. Yang, O. M. Yaghi and C. J. Chang, Science, 2015, **349**, 1208-1213.
- Q. Xu, S. Tao, Q. Jiang and D. Jiang, Angew. Chem.Int. Ed, 2020, 59, 4557-4563.
- S. Wang, H. Li, H. Huang, X. Cao, X. Chen and D. Cao, Chem. Soc. Rev., 2022. 51. 2031-2080.
- (a) H. Furukawa, K. E. Cordova, M. O'Keeffe and O. M. Yaghi, Science, 2013, **341**, 1230444; (b) B. Li, H. Wen, Y. Cui, W. Zhou, G. Qian and B. Chen, Adv. Mater., 2016, 28, 8819-8860.
- (a) S. Kandambeth, K. Dey and R. Banerjee, J. Am. Chem. Soc., 2019, **141**, 1807–1822; (b) S. B. Alahakoon, S. D. Diwakara, C. M. Thompson and R. A. Smaldone, Chem. Soc. Rev., 2020, 49, 1344-1356.
- (a) Z. Zhang, Y. Ye, S. Xiang and B. Chen, Acc. Chem. Res., 2022, 55, 3752-3766; (b) R.-B. Lin and B. Chen, Chem, 2022, 8, 2114-2135.
- J. Han, J. Feng, J. Kang, J.-M. Chen, X.-Y. Du, S.-Y. Ding, L. Liang and W. Wang, Science, 2024, 383, 1014-1019.
- 10 F. Haase and B. V. Lotsch, Chem. Soc. Rev., 2020, 49, 8469–8500.
- 11 J. Samanta, Y. Zhang, M. Zhang, A. D. Chen and C. Ke, Acc. Mater. Res., 2022, 3, 1186-1200.
- 12 M. Zhang, J. Samanta, B. A. Atterberry, R. Staples, A. J. Rossini and C. Ke, Angew. Chem. Int. Ed., 2022, 61, e202214189.
- 13 R. Liang, J. Samanta, B. Shao, M. Zhang, R. J. Staples, A. D. Chen, M. Tang, Y. Wu, I. Aprahamian and C. Ke, Angew. Chem. Int. Ed., 2021, 60, 23176-23181.
- 14 F. Li, E. Li, K. Samanta, Z. Zheng, L. Wu, A. D. Chen, O. K. Farha, R. J. Staples, J. Niu, K. Schmidt-Rohr and C. Ke, Angew. Chem. Int. Ed., 2023, 62, e202311601.
- 15 (a) E. Li, K. Jie, Y. Zhou, R. Zhao and F. Huang, J. Am. Chem. Soc., 2018, 140, 15070-15079. (b) E. Li, K. Jie, Y. Fang, P. Cai and F. Huang, J. Am. Chem. Soc., 2020, 142, 15560-15568. (c) E. Li, W. Zhu, S. Fang, K. Jie and F. Huang, Angew. Chem. Int. Ed., 2022, 61, e202211780.
- Y. Zhang, R. Liang, B. A. Atterberry, F. Li, R. J. Staples, J. Zhang, J. Samanta, A. J. Rossini and C. Ke, J. Am. Chem. Soc., 2024, 146, 15525-15537.
- 17 H. Wu, L. Zhang, Y. Xu, Z. Ma, Z. Shen, X. Fan and Q. Zhou, J. Polym. Sci. Part A: Polym. Chem., 2012, 50, 1792-1800.
- 18 J. W. McCutcheon, Ind. Eng. Chem. Anal. Ed., 1940, 12, 465-465.

Journal Name ARTICLE

Table of Contents

